Available online at www.sciencedirect.com
ScienceDirect
Journal of the European Ceramic Society 31 (2011) 391–400
www.elsevier.com/locate/jeurceramsoc

Effect of single-walled carbon nanotubes on thermal and electrical properties of silicon nitride processed using spark plasma sintering

Erica L. Corral [a,*,1], Hsin Wang [b], Javier Garay [c], Zuhair Munir [d], Enrique V. Barrera [e]

[a] The University of Arizona, Materials Science & Engineering Department, 1235 James E. Rogers Way, Tucson, AZ 85721, USA
[b] Oak Ridge National Laboratory, Materials Science and Technology Division, P.O. Box 2800, Oak Ridge, TN 37831, USA
[c] University of California at Riverside, Riverside, CA, USA
[d] University of California at Davis, Chemical Engineering and Materials Science Department, 1 Shields Ave., Davis, CA 95616-5294, USA
[e] Rice University, Department of Mechanical Engineering and Materials Science-MS 321, P.O. Box 1892, Houston, TX 77251, USA

Received 23 July 2010; received in revised form 5 October 2010; accepted 11 October 2010

Abstract

Si_3N_4 nanocomposites reinforced with 1-, 2-, and 6-vol% single-walled carbon nanotubes (SWNTs) were processed using spark plasma sintering (SPS) in order to control the thermal and electrical properties of the ceramic. Only 2-vol% SWNTs additions were used to decrease the room temperature thermal conductivity by 62% over the monolith and 6-vol% SWNTs was used to transform the insulating ceramic into a metallic electrical conductor (92 S m^{-1}). We found that densification of the nanocomposites was inhibited with increasing SWNT concentration however, the phase transformation from α- to β-Si_3N_4 was not. After SPS, we found evidence of SWNT survival in addition to sintering induced defects detected by monitoring SWNT peak intensity ratios using Raman spectroscopy. Our results show that SWNTs can be used to effectively increase electrical conductivity and lower thermal conductivity of Si_3N_4 due to electrical transport enhancement and thermal scattering of phonons by SWNTs using SPS.

Keywords: Single-wall carbon nanotubes; High-temperature materials; Thermal properties; Electrical properties; Composites

1. Introduction

SWNTs are considered to be ideal fiber reinforcements for the creation of multifunctional nanocomposites with enhanced fracture toughness and strength, and enhanced electrical and thermal conductivities in polymeric, ceramic, and metallic based nanocomposites.[1–4] SWNTs possess exceptional mechanical ($E > 1$ TPa and TS > 7 GPa)[5] thermal ($k \sim 1750$–5800 W m^{-1} K^{-1}),[5–7] and electrical properties ($\sigma \sim 10^6$ S m^{-1})[5,8] and have considerably high aspect ratios (1,000 up to 10,000) that are critical for their use in the design of nanocomposites. SWNTs have high electrical conductivity along the tube axis and depending on the type of the arrangement of bond structure chirality within the nanotube, a SWNT can be either metallically conducting or semiconducting. Experimental results show that a SWNT rope has a longitudinal electrical conductivity of 10^6 S m^{-1} at 300 K.[5,9] Theory predicts high thermal conductivity values (5800 W m^{-1} K^{-1}) for the room temperature longitudinal thermal conductivity of an individual SWNT.[7] However, experimental measurements of aligned bundles of SWNTs showed a measured thermal conductivity of only 250 W m^{-1} K^{-1} at room temperature.[8] Although, SWNTs have high thermal conductivity, it is very difficult to realize this effect in a composite. This is mainly because SWNTs are not continuous throughout the bulk composite. Therefore, they create more interfacial defects, which may lower the lattice thermal conductivity. In addition, depending on the SWNT synthesis method, lot-to-lot variability, chirality of the structure, defects, and single vs. bundles of SWNTs there are a number of additional variables that make it difficult to fully understand the effect of SWNTs on thermal and electrical properties when used as additives in nanocomposites. Clearly, ongoing efforts focused on enhancing the production quality, length scale, chiral structure and defects, and quantity of SWNTs[9–12] will

* Corresponding author.
E-mail address: elcorral@email.arizona.edu (E.L. Corral).
[1] Based in part on dissertation submitted by E.L. Corral for a Ph.D. in Materials Science at Rice University, Houston, TX, 2005.

0955-2219/$ – see front matter © 2010 Elsevier Ltd. All rights reserved.
doi:10.1016/j.jeurceramsoc.2010.10.020

help promote an understanding of their effects in nanocomposite systems. Once, continuous and uniform SWNTs are processed into a composite will the potential for enhanced thermal conductivity properties be realized and may lead to the use of SWNTs for high-performance thermal management systems.

The vast majority of SWNT nanocomposites have been focused on polymeric systems due to favorable processing methods that allow chemical handling of each material at room or low temperature conditions. However, for both metal and ceramic nanocomposite development the challenge lies with incorporating SWNTs at high temperature either though conventional melting casting or sintering methods. This becomes a significant hurdle to overcome when SWNTs are not stable at high temperatures >600 °C (in air)[13] and oxidize. Therefore, exposing SWNTS to extreme temperatures (>1800 °C) and pressures (50 MPa) using conventional ceramic sintering methods puts them at higher risk for oxidation and structural damage. The challenge for researchers to process SWNTs in high-temperature ceramic matrices such as, carbides, nitrides, and borides, is primarily during sintering where temperature requirements usually exceed 1800 °C, using conventional sintering methods.[14–16] In addition, creating processing methods that enable homogeneous dispersions of SWNTs and ceramic particles is critical for obtaining uniform densification and physical properties of the ceramic nanocomposites. The most promising method for dispersing SWNTs in a ceramic is to use colloidal processing in order to manipulate interparticle pair potential in order to create homogeneous aqueous or solvent based dispersions of powders and SWNTs. Our previously published work[14] and work published by others[17–19] has shown that colloidal processing methods are highly effective in obtaining well dispersed homogeneous SWNTs in oxide and non-oxide ceramics. The basis for this approach is to treat the ceramic particle and the SWNT as a colloid particle and employ conventional colloidal processing methods that involved manipulating the inter-particle and inter-tube pair potentials.[20]

Despite the processing challenge presented by creating ceramic nanocomposites and the variability between individual and bundles of SWNTs there have been promising results for oxide and non-oxide based SWNT ceramic nanocomposites. Recent work by others and us shows the potential to enhance toughness of brittle ceramics and to tailor their electrical and thermal conductivity properties.[4,16,21–24] For example, the SWNT–Al_2O_3 nanocomposites processed using SPS and conventional ceramic powder mixing/blending methods have shown to increase fracture toughness by 30%,[22] while also creating a metallic electrically conductive ceramic with anisotropic thermal properties.[23] In addition, Balani et al.[25,26] enhanced the fracture toughness of alumina by 42% over the monolith. Recently, the work by Zhang et al.[19] has shown for the first time that pressure-less sintering can be used to densify and consolidate MWNT-Al_2O_3 nanocomposites at 1500 °C for 2 h and obtain ~99% theoretical density without detectable damage to the MWNT structure. Their results also show modest enhancements to fracture toughness due to pull out of the MWNTs and significant increases in flexural strength over the monolith. Recently, Inam et al.[27] reported that using 5-wt% MWNTs in Al_2O_3 they were able to create excellent electrical conductors with conductivity values greater than 500 S m^{-1}.

However, there has been limited success in creating ceramic nanocomposites with significant enhancements to thermal conductivity, which is an important physical property that helps us understand how heat transfers through a solid. Bakshi et al.[28] were able to enhance the thermal conductivity of Al_2O_3 coatings using 4-wt% MWNTs. Also, Sivakumar et al.[29] reported a 70% increase in thermal conductivity of SiO_2 using 10-vol% MWNTs. However, the improvements they measured fall short of the enhancements predicted by rule of mixtures calculations. On the other hand, Zhan et al.[21] observed a decrease in thermal conductivity with increasing vol% SWNT. There are a number of reasons for the lower thermal conductivity values that take into consideration that SWNT bundles have lower thermal conductivity values than individual SWNTs and that the number of interfaces between the Al_2O_3 and the SWNTs creates high thermal resistivity thus limiting thermal conduction in the nanocomposites. It is also important to note that residual porosity within the ceramic nanocomposite also serves to scatter phonons and limit thermal conduction within a ceramic.

Our previous work shows we can enhance the fracture toughness of Si_3N_4 by 30% upon optimization of SWNT concentration (2-vol% SWNT) and SPS temperature (1600 °C).[14] In addition, others have published results for MWNT reinforced Si_3N_4 showing that for high concentrations of MWNTs (>4 wt%) they react to form SiC thus decreasing the density of the nanocomposite. However, using a lower concentration of MWNTs they were able to maintain the high strength and toughness of the monolith.[16] Thus, the main challenge with processing non-oxide based MWNT or SWNT reinforced ceramic nanocomposites in addition to dispersion of the nanotubes is achieving high density after high-temperature and high pressure assisted sintering. Furthermore, Balazsi et. al.[30] processed MWNT based Si_3N_4 nanocomposites using SPS and hot-pressing and report that the SPS method is superior to hot-isostatic pressure assisted sintering method in obtaining high density and MWNT damage-free structures in Si_3N_4. They also created MWNT–Si_3N_4 nanocomposites with electrical conductivity values greater than 100 S m^{-1}. Recently, SPS has been shown to be a very powerful tool to develop functionally graded and MWNT based nanocomposites. Belmonte et al.[31] have shown that they can process high density nanocomposites and show that SPS can be used to limit MWNT degradation at temperature and that SPS is a powerful tool to develop silicon nitride with controlled microstructures.[32]

The goal of this paper is to investigate the effect of SWNTs on the electrical and thermal properties of Si_3N_4 after densification using SPS. The purpose of the manuscript is to discuss the effect of SPS temperature on SWNT stability at high-temperatures (>1700 °C) and demonstrate that our approach that uses colloidal processing and SPS is successful in retaining pristine and dispersed SWNTs in the sintered microstructure that allow for the enhancement and decrease of the electrical and thermal conductivity properties, respectively.

2. Materials and experimental methods

All of the nanocomposite and monolith specimens were made from powders that were dispersed using colloidal processing methods (as described in detail in our previous published work[14] and as an approach used by others[17]) followed by SPS. The starting Si_3N_4 powders are α-phase content > 90 mass%, with an average particle size of 0.96 μm and <10 mass% sintering additives (Y_2O_3, MgO and Al_2O_3). Commercially available SWNTs (Carbon Nanotechnologies Inc., Houston, TX, USA), in powder form and purified to less than 2-wt% residual metal catalyst were used as received. The nanocomposites made in this study each contain a mixture of well-dispersed single and bundled SWNTs. A cationic surfactant, cetyltrimethylammonium bromide (C_{16}TAB) (Sigma–Aldrich Corp., St. Louis, MO, USA) was used as a dispersant throughout this study. We used SPS (Dr. Sinter SPS-1050, Sumitomo Coal Mining Co. Ltd., Tokyo, Japan) to densify our nanocomposites using a maximum pulse current of 5000 A and maximum pulse voltage of 10 V. The pulse cycle was 12 ms on and 2 ms off with a heating rate of 200 °C min^{-1}. The temperature was monitored on the surface of the die wall using optical pyrometry. It has been experimentally estimated that the die surface temperature and the powder compact temperature can be up to 150 °C off the set-point temperature. An external pressure of 25 kN was applied as the powders were heated inside a graphite die lined with graphite foil to prevent surface reactions between the powder and the inner die wall. A vacuum of 10^{-2} Torr was used and sintering occurred under vacuum.

Bulk densities (ρ) were measured using the Archimedes method. Phase identification of the sintered materials was performed by X-ray diffractometry (XRD) and the relative content of α/β phase in the dense bodies was determined from the relative intensities of selected diffraction peaks.[33] Structural characterization of SWNT after high temperature sintering in a ceramic was performed using Raman spectroscopy. The sintered microstructures were examined by scanning electron microscopy (SEM, JEOL 6500F, JEOL USA Inc., Peabody, MA).

The thermal diffusivity (α) of the monolith and composites were measured from room temperature to 1000 °C, by laser-flash method, using a thermal-constant analyzer (FL5000, Anter Corporation, Pittsburgh, PA). To evaluate the thermal diffusivity, 20 mm diameter and 3 mm thick disc specimens were used. The thermal conductivity κ at room temperature was calculated using the equation:

$$\kappa = \alpha C_P \rho.$$

The room temperature specific heat (C_P) of the specimens was calculated using the rule of mixtures for SWNT–Si_3N_4 composites. We did not measure room temperature or at temperature specific heat values. The room temperature specific heat values calculated were 0.67, 0.6502, 0.6504, and 0.6512 J g^{-1} K^{-1} for 0, 1, 2 and 6-vol% SWNT nanocomposites were used to calculate room temperature thermal conductivity values. Room temperature electrical conductivity (σ) measurements of the SWNT–Si_3N_4 nanocomposites were made using a four-point probe technique, in observation with ASTM B193-02, using a combination of volt-meters (Hewlett-Packard 4339A, High Resistance Meter (Agilent 345A 81/2 Digital Multimeter).

3. Results

3.1. Spark plasma sintering of silicon nitride and SWNT–Si_3N_4 nanocomposites

High-density monolithic ceramics and nanocomposites were obtained using SPS as seen in Table 1. The monolithic ceramic density values averaged around 95% theoretical density (T.D.) when sintered at 1600, 1700 or 1800 °C (0- or 3-min hold time) where the highest density monolith (97% T.D.) was sintered at 1800 °C, 3-min hold. Shrinkage displacement profiles obtained

Table 1
Sintering density and electrical and thermal properties for Si_3N_4 and SWNT–Si_3N_4 nanocomposites, measured and calculated at room temperature.

Material	SPS temp. (°C)	SPS time (min)	Theoretical density (%)	Electrical conductivity (S m^{-1})	Thermal diffusivity (cm^2 s^{-1})	Thermal conductivity (W m^{-1} K^{-1})
Si_3N_4	1600	0	96.4	3.1E−11	0.075	15.77
	1600	3	93.1	3.6E−11	0.120	24.15
	1700	0	95.0	8.0E−11	0.080	16.47
	1700	3	94.2	3.0E−11	0.136	27.70
	1800	3	97.2	1.5E−11	0.112	23.49
1.0 vol%	1300	3	82.5	6.2E−6	0.037	5.22
	1600	0	87.3	1.8E−9	0.062	11.38
	1600	3	95.4	4.7E−5	0.065	12.93
	1690	0	95.0	1.8E−8	0.101	20.06
2.0 vol%	1300	3	82.5	4.4E−6	0.050	8.642
	1600	0	91.0	4.7E−5	0.066	12.42
	1600	3	90.5		0.107	20.16
	1680	0	96.6	1.8E−8	0.065	13.07
6.0 vol%	1300	3	76.5	22.01	0.043	6.78
	1600	3	91.0	91.91	0.077	14.40
	1800	0	84.3	0.69	0.059	10.14

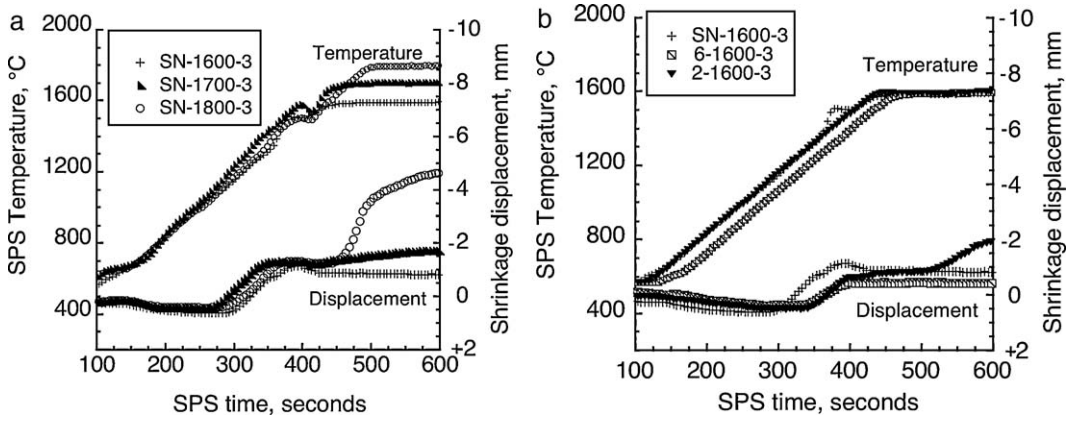

Fig. 1. Shrinkage displacement curves for Si_3N_4 and SWNT–Si_3N_4 nanocomposites during SPS show rapid densification. SPS shrinkage curves for material sintered at temperature for 3 min (a) for the monolith material at temperatures of 1600, 1700, and 1800 °C, and (b) for the nanocomposites at 1600 °C for 0, 2, and 6-vol% SWNT concentrations.

during SPS for the monoliths at 1600, 1700, and 1800 °C (3-min hold) are shown in Fig. 1(a). As expected, the degree of shrinkage displacement increases with increasing temperature up to 1800 °C. The 1800 °C shrinkage displacement curve undergoes a high temperature conversion from α to β Si_3N_4 which is indicated by the steep shrinkage curve that is absent during lower temperature sintering runs.

The nanocomposites (1-, 2-, and 6-vol% SWNT) density values averaged to be approximately 91% theoretical density (T.D.) when sintered at 1600, 1700 or 1800 °C (0- or 3-min hold time). The highest density nanocomposite values (∼98% T.D.) were obtained using 2-vol% SWNT and sintered at 1680 °C (0-min hold). However, increasing SWNT content from 1- or 2-vol% SWNT to 6-vol% SWNT decreases the average nanocomposite density values from, 93% to 88% T.D., respectively. As expected as the sintering temperature increases the overall density for the nanocomposites increases except for the 6-vol% SWNT nanocomposite system which decreases in density with increasing temperature.

Shrinkage displacement profiles measured during SPS for the monolith, 2-vol% SWNT, and 6-vol% SWNT nanocomposites (1600 °C for 3-min hold time) are shown in Fig. 1(b). Clearly, the shrinkage displacement profiles show that the time for densification or shrinkage to take place increases as the SWNT concentration increases in the nanocomposite. However, the 2-vol% SWNT nanocomposite undergoes a steady increase in displacement over time at temperature and the 6-vol% nanocomposite does not increase shrinkage displacement upon reaching the final sintering temperature. This is likely due to the fact that the 6-vol% SWNT nanocomposites powders were not well dispersed due to the difficulty in using colloidal processing to disperse a high concentration of nanosize fibers thus, limiting densification. As expected, a high concentration of SWNTs inhibits densification of the ceramic because they act as physical barriers to sintering.

3.2. Microstructure and crystal structure of sintered nanocomposites

Scanning electron micrographs for the 2-vol% SWNT–Si_3N_4 nanocomposites sintered at 1300 and 1600 °C are shown in Fig. 2(a) and (b), respectively. The micrographs show that SWNTs are homogeneously dispersed throughout the sintered matrices. The 1300 °C sintered nanocomposite has a matrix composed of α-Si_3N_4 which has an equiaxed grain structure (Fig. 2(a)). The 1600 °C nanocomposites has a mixture of α- and β-Si_3N_4, which is mixture of equiaxed and rod-like grain structures (Fig. 2(b)).

XRD was used to confirm and fully characterize the α–β phase transformation for the monolith (Fig. 3(a)) and a 6-vol%

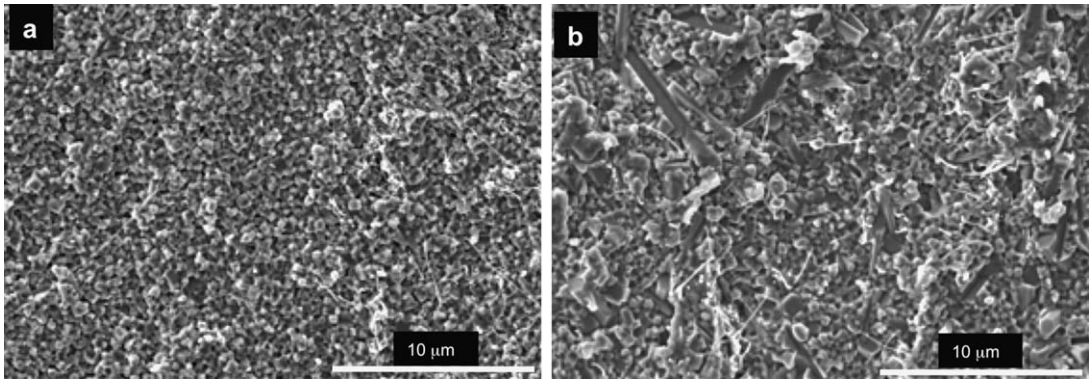

Fig. 2. Representative scanning electron micrographs for 2-vol% SWNT–Si_3N_4 nanocomposites densified using SPS. The nanocomposites were sintered for (a) 3 min at 1300 °C and (b) 0-min at 1600 °C.

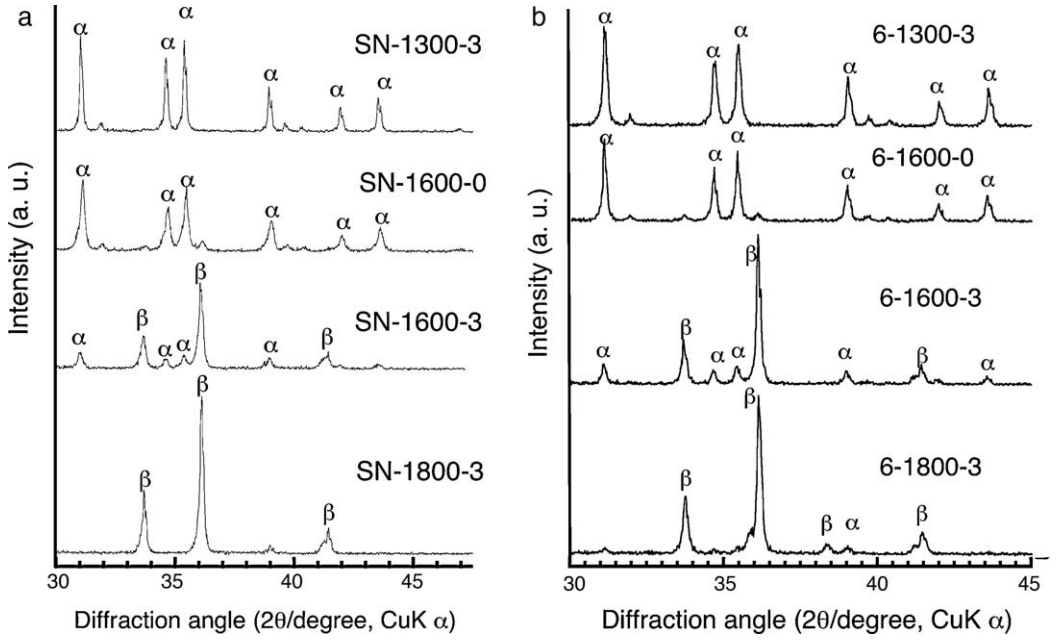

Fig. 3. XRD spectra show phase transformation from a-to-b Si_3N_4 for both Si_3N_4 and SWNT–Si_3N_4 nanocomposites using SPS. XRD spectra for (a) Si_3N_4 and (b) SWNT–Si_3N_4 nanocomposites sintered at 1300, 1600 and 1800 °C from zero to 3 min at temperature.

SWNT–Si_3N_4 nanocomposite (Fig. 3 (b)). The onset of the α- to β-Si_3N_4 phase transformation takes place at the same temperature (1600 °C) for both the nanocomposite and monolithic materials and a mixed α- and β-Si_3N_4 grain structure is produced upon holding the temperature at 1600 °C for 3 min. Therefore; SWNTs do no impede Si_3N_4 phase transformation at temperature and phase transformation results are very reproducible and accurately controlled using SPS. XRD analysis also showed that after SPS at 1300 °C (0-min hold) and 1800 °C (3-min hold) both systems were 100% α-Si_3N_4 and 100% β-Si_3N_4, respectively. The XRD spectra for the 6-vol% SWNT nanocomposites does not show any SiC peaks suggesting that the sintering procedure did not result in any considerable reactions between SWNTs and Si_3N_4 at temperature (up to 1800 °C).

3.3. Raman spectroscopy of SWNT–Si_3N_4 nanocomposites after SPS

Our previously work shows that evidence of SWNTs was found in the ceramic after SPS as high as 1800 °C.[14] In this study we take a closer look at the affect of SPS temperature and time on the structure of SWNTs within a sintered Si_3N_4 nanocomposite as shown in Fig. 4. The SWNT Raman spectrum has four characteristic bands three of which are described here: a radial breathing mode (100–300 cm^{-1})[34,35] a tangential mode (G-band, 1500–1600 cm^{-1}),[34,35] and a D mode,[34,35] as seen in Fig. 4(a). The defect-induced D mode originates from double-resonant Raman scattering[35] that is likely a result of impurities or defects in the crystalline structure. However, the peak shape is indicative of metallic or semiconducting nature of the tubes and the SWNTs used in this study indicate they are primarily conductive SWNTs with some structural defects due to processing, as indicated by the small defect peak at 1300 cm^{-1}. Raman spectroscopy was used to characterize the as-received SWNT material (Fig. 4(a)), the affect of SWNT concentration for a given sintering temperature (1600 °C) and time (3-min) (Fig. 4(b)), and the affect of SPS temperature for a given SWNT concentration (Fig. 4(c)). As expected, Fig. 4(b) shows that the intensity of the SWNT peaks increase with increasing SWNT concentration from 1- to 2- to 6-vol% SWNT nanocomposites. Fig. 4(c) shows that as sintering temperature increases, from 1300 °C to 1600 °C (2-vol% SWNT–Si_3N_4 nanocomposites) the SWNT peak intensities decrease. It also shows that the SWNT peak intensity decreases as you increase time at temperature from a 0-min to a 3-min hold, at 1600 °C. Therefore, the effect of SPS time and temperature indicate that in order to retain the as-processed concentration of SWNTs without sintering induced structurally damaged that the lowest temperature and shortest times at temperature will ensure the least amount of sintering damage onto the SWNTs.

In order to quantify the amount of structural damage introduced to the SWNTs after high-temperature sintering, we calculated the D:G ratios taken from measured Raman intensities for both as-received SWNTs and for SWNTs in the final sintered microstructures (Fig. 4). The calculated ratio indicates the degree of structural damage in the SWNTs, either as a result of their production synthesis or, in this case, from SWNT synthesis and subsequent high-pressure and high-temperature sintering within a nanocomposite. The type of structural damage can either be atomic defects in the structure or imperfections in crystal order.[11] The higher the D:G ratio the greater degree of structural damage to the SWNTs. As-received SWNTs have a D:G ratio of 0.108, which indicates that the synthesized and purified material contained some random disorder in the SWNT structure from the production process.[36] Therefore, the baseline D:G ratio used to compare against the SWNTs in the sintered

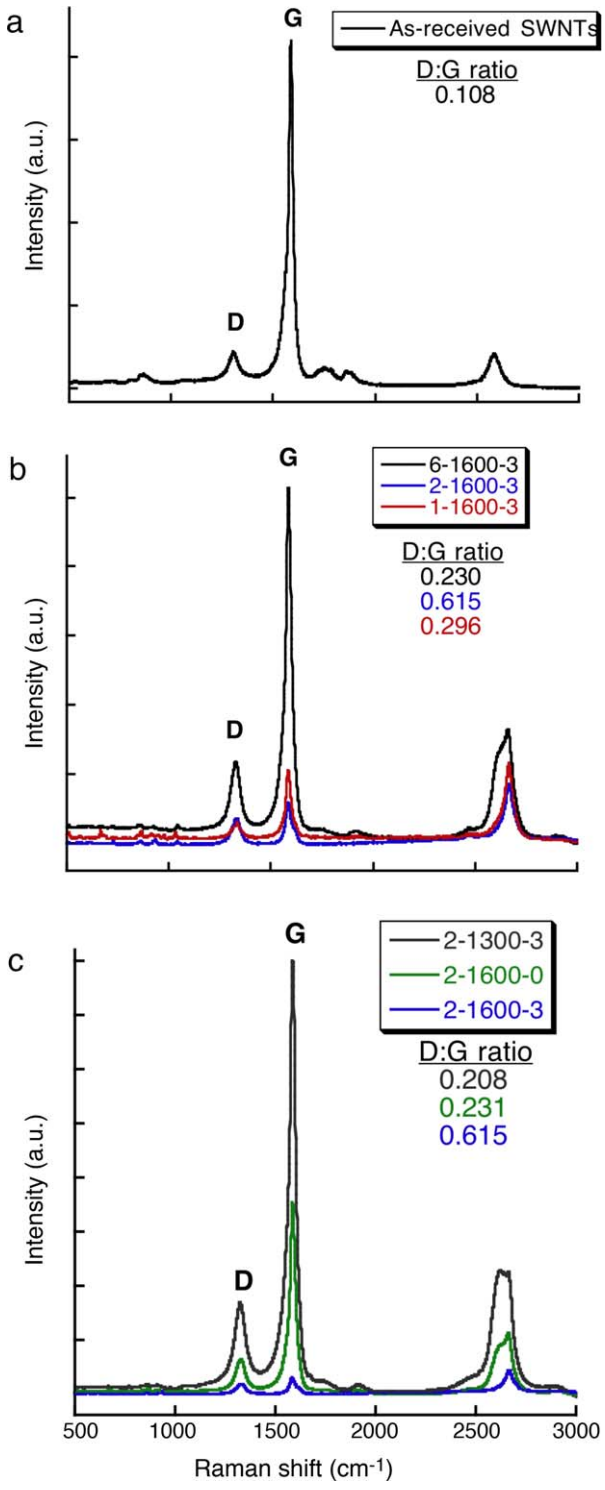

Fig. 4. Raman spectroscopy shows SWNTs survive high temperature sintering using SPS for (a) as-received SWNTs before processing into nanocomposites (b) 1, 2, and 6-vol% SWNTs sintered at 1600 °C for 0 min and for (c) 2-vol% SWNT nanocomposites sintered from 1300 to 1600 °C.

nanocomposites will be 0.108. The D:G ratios calculated for the nanocomposites sintered at 1600 °C (3-min hold) with increasing SWNT concentration (from 1-, 2- and 6-vol% SWNT) were calculated to be, 0.296, 0.615, and 0.230, respectively. The nanocomposite with the highest calculated degree of structural damage was the 2-vol% SWNT nanocomposite (D:G = 0.615). However, the D:G ratios for the other two composites, 1- and 6-vol% SWNT nanocomposites, sintered at the same temperature and time have considerably lower D:G ratios between 0.296 and 0.230, respectively. These calculated D:G ratios do not follow a trend that results in an increased amount of structural damage with increasing SWNT concentration. Rather, these results suggest that there is variability between the nanocomposite powders processed prior to sintering that may influence localized heating mechanisms during SPS if the powder mixtures containing SWNTs are not well dispersed. Now, if we look at the effect of SPS temperature and SPS time at temperature on the D:G ratio for the 2-vol% SWNT nanocomposite we see a clear trend that quantifies structural damage with sintering conditions (Fig. 4(c)). For example, the D:G ratios increase in intensity from, 0.208 to 0.23, with increasing temperature from, 1300 to 1600 °C (0-min hold). In addition, the D:G ratios increase in intensity from, 0.231 to 0.615, with increasing time at temperature (1600 °C) from 0- to 3-min hold, respectively. These results suggest that SPS can be used to obtain high-density nanocomposites with little structural damage. However, there seems to be variability between SPS runs that are most likely due to powder mixture dispersion levels and variability of SWNTs that result in significant structural damage to the SWNTs after sintering. Monitoring D:G ratios may be useful for verifying the quality of the SPS processing run and may be helpful in assessing overall nanocomposite processing integrity.

3.4. Electrical properties of SWNT–Si_3N_4 nanocomposites

Table 1 shows the measured and calculated room temperature electrical conductivity values for the monolith and 1-, 2- and 6-vol% SWNT nanocomposites. It is well known that sintered silicon nitride is an excellent electrical insulator ($s \sim 10^{-12}$ S m^{-1}). Our monolithic materials have an average electrical conductivity value of 4.6×10^{11} S m^{-1}, which is considered to be an insulator. This value increases towards electrical conductivity with increasing SWNT concentration from, 1-, 2- and 6-vol% SWNT, with average electrical conductivity values of, 1.33×10^{-5}, 1.71×10^{-5}, and 57.0 S m^{-1}, respectively. Therefore, using up to 6-vol% SWNTs results in the transformation of the ceramic insulator into a metallic conductor. The highest room temperature electrical conductivity value measured was 92 S m^{-1} for the 6.0-vol% SWNT nanocomposite. This value lies near the low end for room temperature metallic conductive materials[37] where copper is at the high end with an electrical conductivity value of 59.6×10^6 S m^{-1}. A plot of the average room temperature electrical conductivity as a function of SWNT concentration (Fig. 5(a)) shows that we were able to change the insulator into a semi-electrically conducting material using 2-vol% SWNTs. This plot also suggests that there exists an electrical conduction percolation threshold between 2- and 6-vol% SWNTs that will impart electrical conductive properties within the ceramic. Fig. 5(b) shows the range of room temperature electrical conductivity values for each SWNT nanocomposite as a function of SPS sintering temperature. This plot shows that the 6-vol% SWNT nanocomposite has the high-

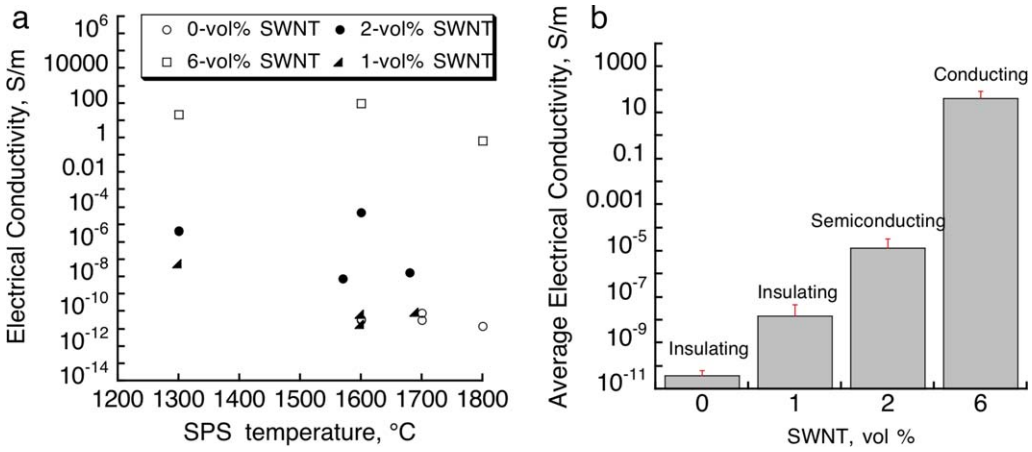

Fig. 5. Room temperature electrical conductivity values measured for Si_3N_4 and SWNT–Si_3N_4 nanocomposites as function of (a) SPS temperature and (b) SWNT vol%.

est overall measured electrical conductivity values than the 1- or 2-vol% SWNT nanocomposites as a function of sintering temperature from 1300, 1600 and 1800 °C. As the temperature increases from 1600 to 1800 °C the electrical conductivity drops significantly. The same observation is made for the 1- and 2-vol% SWNT nanocomposites. These values also suggest that the electrical conductivity values are more sensitive to SWNT concentration than SPS sintering temperature.

3.5. Thermal properties of SWNT–Si_3N_4 nanocomposites

Table 1 shows the measured room temperature thermal diffusivity values and calculated thermal conductivity values for the monolith and 1-, 2- and 6-vol% SWNT nanocomposites. The average thermal conductivity value for the monoliths is 21.4 $W\,m^{-1}\,K^{-1}$. This average value decreases independent of SWNT concentration (1-, 2- and 6-vol% SWNT) to average thermal conductivity values of, 12.4, 13.5, and 10.4 $W\,m^{-1}\,K^{-1}$, respectively. Therefore, on average the room temperature thermal conductivity value of the monolith decreases by, 57.9%, 63.1% and 48.6%, for the 1-, 2-, and 6-vol% SWNT nanocomposites, respectively. However, the average room temperature and subsequent high temperature thermal conductivity values reported here were measured on less than 100% dense nanocomposites. Therefore, we must contribute a fraction of the lower thermal conductivity properties to be from porosity but when compared to the monolithic materials that also contain residual porosity the effect of pores on the thermal properties is negligible. Our measured room temperature thermal conductivity properties suggest that by adding less than 1-vol% SWNTs to a ceramic you can significantly lower the thermal conductivity of the ceramic, nearly 50% reduction.

We also investigated high temperature thermal diffusivity from room temperature up to 1000 °C for the highest density ceramics and nanocomposites, as seen in Fig. 6(b). As expected, the thermal diffusivity values for the monolith and the nanocomposites follow the same general trend that shows a steady decrease in thermal diffusivity with increasing temperature. However, the nanocomposites have a considerably lower starting thermal diffusivity value than the monolith and maintain the same level of lower thermal diffusivity values than the monolith with increasing temperature up to 800 °C. At temperatures equal or greater than 800 °C the thermal diffusivity values of the monolith and the nanocomposites converge to very similar values. These results suggest that the SWNTs can tailor thermal diffusivity and thermal conductivity properties in ceramics up

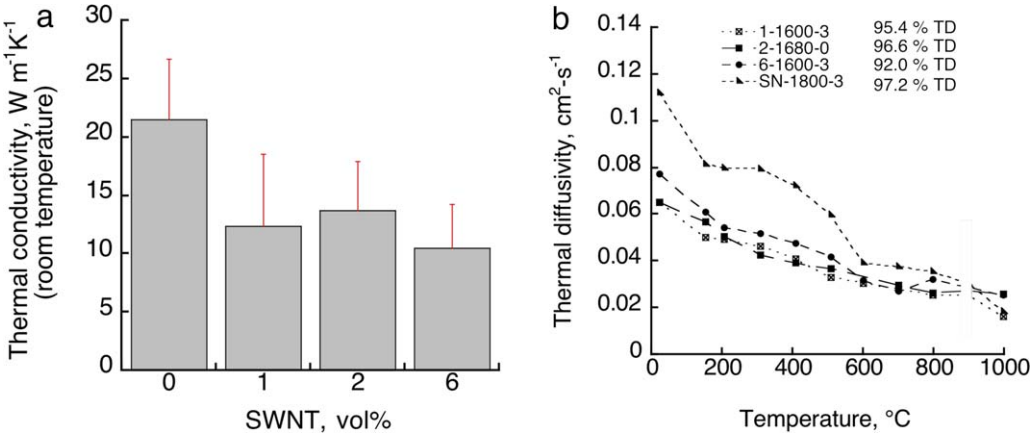

Fig. 6. (a) Room temperature thermal conductivity values decrease with small additions of SWNTs to the ceramic. (b) Thermal diffusivity values measured from room temperature to 1000 °C for high-density monolithic ceramic, and for the 1, 2, and 6-vol% SWNT nanocomposites.

to high temperatures. However, in order to fully understand the effect of SWNTs on thermal and electrical properties in ceramics requires further investigation at high temperatures.

4. Discussion

The ability to manage electrical and thermal conductivity properties in ceramics has widespread use for application at high temperature as smart skins, stress sensors, and thermal management materials. However, in order to realize these materials in application we need to further investigate the effects of processing SWNTs in ceramics and how they affect the electrical and thermal properties of the ceramic. For this study we focused on investigating both electrical and thermal properties of a high temperature ceramic that contain a homogeneous random dispersion of SWNTs. Our results shows that SWNTs can be used to effectively tailor both electrical and thermal properties of silicon nitride. However, as the nanocomposite room temperature electrical conductivity increases with increasing SWNT addition, the opposite trend is observed for thermal conductivity properties. Some factors effecting the modest enhancement of electrical conductivity can be related to nanocomposite powder processing and sintering methods. Our previously published work[14] and work published by other groups[17] shows that colloidal processing methods are very effective in creating homogenously dispersed SWNT–ceramic nanoparticle suspensions and that the SWNT dispersion level is retained within the final sintered microstructure. However, the effect of high temperature pressure assisted sintering on the stability of the SWNT structure is not well understood because researchers have used different sintering methods and maximum temperatures. The SWNTs in this study were dispersed using colloidal processing methods and the dispersion state was retained after sintering which is also verified by our measured electrical resistivity results that show enhancements to electrical conductivity of the ceramic likely due to a homogeneous dispersion of SWNTs. In addition, the argument can be made that the better the dispersion level the less likely that there are large agglomerated bundles of SWNTs throughout the ceramic or that the SWNT bundles are restricted to locations around the grain boundaries. The latter case would result in higher electrical conductivity results. Our electrical conductivity results are lower than other reported nanocomposites processed using conventional powder mixing techniques because the SWNT dispersion is not restricted to only the grain boundaries but are also found within the grains of silicon nitride. When SWNTs are present in a material above the percolation limit, they also provide a continuous electrical conduction path that are not dependent on SWNT alignment or orientation within the matrix therefore, this homogeneous and random distribution of SWNTs in the ceramic leads a systematic increase in electrical conductivity.[23]

The interesting phenomenon observed in these novel nanocomposites is that we see opposite effects on electrical and thermal properties with small additions of SWNTs. The high thermal conductivity values for SWNTS in the axial direction should increase the overall thermal conductivity when used in a composite but instead the thermal conductivity is reduced by at least 50% over the monolithic ceramic, while the electrical conductivity seems to increase with increasing SWNT concentration. Although conventional wisdom would indicate that for almost all materials, electrical and thermal conductivities move in the same direction it is believed that the introduction of SWNTs into ceramics increases the number of phonon scattering points, thereby lowering the thermal conductivity of the ceramic.[15] Thermal conductivity can be expressed as the sum of lattice thermal conductivity (by phonons) and electronic thermal conductivity (by electrons or holes): $K(\text{total}) = K(\text{lattice}) + K(\text{electronic})$. We observed adding SWNTs into Si_3N_4 increased electronic component of the thermal conductivity and in the meantime lower the lattice thermal conductivity. The net effect of much lower thermal conductivity indicates that lattice thermal phonon scattering at the interfaces reduced conductivity significantly. We also have take into consideration that the SWNTs are randomly and homogeneously dispersed throughout the matrix material therefore, the transverse thermal conductivity properties which are significantly lower than their axial thermal conductivity properties also contribute to the lower than expected thermal conductivity properties. In order to take advantage of the high thermal conductivity properties in a ceramic the SNWTs have to be aligned through the matrix and not randomly homogeneously dispersed as in our present study. This increase in electrical conductivity should also increase thermal conductivity but instead they decrease due to differences in anisotropic thermal properties between individual tubes and bundles of tubes.[6] In addition, numerous highly resistive thermal junctions between the tubes can contribute to additional extrinsic phonon scattering mechanisms such as tube–tube interactions that are barriers to thermal transport in ropes of nanotubes.[38] It can also be assumed that the inter-tube coupling in ropes is strong, based on mechanical properties and enhanced electrical properties reported for SWNT reinforced-alumina composites processed using SPS.[14,22,23] In addition, microstructural observations indicate that SWNT ropes are intertwined with Si_3N_4 grains, suggesting that a significant degree of curvature or bending occur in the bundles that may decrease thermal flux properties in the SWNTs.[21] The potential to enhance the thermal conductivity of the ceramic may be possible if methods can be developed to align SWNT bundles within the bulk nanocomposite. It should be noted that there has only been one published report[41] that shows an increase in thermal conductivity for carbon nanotube reinforced Si_3N_4 ceramic nanocomposites using MWNTs as reinforcements. The nanocomposite system was processed using a different method that was not colloidal processing and results in different microstructures than those observed in this study. However, for the MWNT–Si_3N_4 system there was a measured 4% increase in thermal conductivity at 200 °C.

The composites processed using SPS experienced a hot-pressing stress during consolidation that produce a mechanical stress on the SWNTs in the axial (hot-pressing) direction. Others have reported that this leads to lower thermal conductivity values in the transverse direction for SWNT–alumina composites at concentrations greater than 10-vol% SWNTs.[21] Our thermal diffusivity measurements conducted in the transverse direction, at

room temperature, for the SWNT–Si_3N_4 nanocomposites were the same in the axial direction. Therefore, a homogenous and random dispersion of SWNTs within the ceramic is believed to be the reason for the consistent thermal measurements for the transverse and axial directions. Thermal diffusivity values measured for the 6-vol% SWNT composite show a small increase in the transverse direction over the axial direction, indicating that there is a critical concentration of SWNTs that can be effectively dispersed homogeneously and otherwise leads to anisotropic behavior in ceramic materials. In addition, SWNTs possess a very high surface area and when they are well dispersed with Si_3N_4 particles the increase in the available interfacial area between SWNTs and between SWNTs and Si_3N_4 particles is substantial. The interface effect, also known as the Kakpitza effect[39] has a tendency to reduce the thermal flux and reduce thermal conductivity for composites. The thermal diffusivity values decrease with the incorporation of SWNTs over the temperature profile tested and all specimens show a decrease in thermal diffusivity with increasing test temperature. These results are consistent with results observed for pure carbon materials.[40] The observed reduction in thermal diffusivity with increasing temperature can be attributed to the dominant effect of Umklapp scattering (phonon–phonon scattering) reducing the phonon mean free path length.[15,40]

Considering the high-temperature and high-pressure sintering conditions that are necessary to densify the monolith it is a very surprising that SWNTs are retained in the final sintered microstructure. However, we found direct evidence using Raman spectroscopy measurements that some or most of SWNTs survived the SPS sintering process. However, comparing the D to G peak ratios we also found that there are some structural defects in the as-received SWNTs and an increase in the ratio was measured after SPS suggesting that there is high a risk to using high temperature that results in an increase in SWNT defects. There is no clear trend that shows increasing D:G ratio with increasing sintering temperature or time. However, this method for characterizing the SWNTs after SPS shows to be useful for helping understand the relationship between nanocomposite powder processing and sintering conditions.

5. Summary

Multifunctional SWNT–Si_3N_4 nanocomposites were processed using 1-, 2-, and 6-vol% SWNTs and densified using SPS. Our previous work has shown these composite have mechanically properties equal to fully sintered Si_3N_4 and under certain processing conditions have the potential to increase the fracture toughness of an already structurally tough ceramic material by 30% over the monolith. The insulating ceramic was transformed into a metallic electrical conductor with a value of 92 S m^{-1} at room temperature. However, our nanocomposites can also be used as thermal management material with up to a 60% reduction in thermal conductivity using small additions of SWNTs. The Raman spectroscopy study showed that SWNTs are retained in the final sintered microstructure. However, we also detected structural damage to the SWNTs as a function of sintering temperature up to 1800 °C. We also report that SPS can be used to successfully process SWNTs in a high-temperature ceramic without a noticeable reaction between SWNTs and the ceramic. SPS also allows for processing high-density nanocomposite with precise control over the phase transformation of the matrix material. Further studies are needed in order to understand the effects of high-temperature and pressure on the structures of SWNTs in a high-temperature ceramic but the initial findings reported here suggest that there is significant potential for these novel nanocomposites in high temperature applications.

Acknowledgements

This work has been financially supported by The Robert Welch Foundation of Texas grant number C1494, the NSF-AGEP at Rice University grant number HRD-9817555, Carbon Nanotechnologies Inc., NASA-URETI grant number NC-01-0203 and NASA Ames Research Center grant number NNA04CK63A. Research at The High Temperature Materials Laboratory (HTML) was sponsored by the Assistant Secretary for Energy Efficiency and Renewable Energy, Office of Vehicle Technologies, as part of the HTML User Program, Oak Ridge National Laboratory, managed by UT-Battelle, LLC, for the U. S. Department of Energy under contract number DE-AC05-00OR22725.

References

1. Thostenson E, Li C, Chou T. Nanocomposites in context. *Composites Science and Technology* 2005;**65**(3–4):491–516.
2. Thostenson E, Ren Z, Chou T. Advances in the science and technology of carbon nanotubes and their composites: a review. *Composites Science and Technology* 2001;**61**(13):1899–912.
3. Ajayan P, Tour J. Nanotube composites. *Nature* 2007;**447**(7148):1066–8.
4. Curtin WA, Sheldon BW. CNT-reinforced ceramics and metals. *Materials Today* 2004;**7**(11):44–9.
5. Meyyappan M. *Carbon nanotubes: science and applications*. Boca Raton: CRC Press LLC; 2005.
6. Hone J, Piskoti C, Zettl A. Thermal conductivity of single-walled carbon nanotubes. *Physics Review B* 1999;**59**(4):R2514–6.
7. Berber S, Kwon Y-K, Tomanek D. Unusually high thermal conductivity of carbon nanotubes. *Physical Review Letters* 2000;**84**(20):4613–6.
8. Hone J, Llaguno MC, Nemes NM, Johnson AT, Fischer JE, Walters DA, et al. Electrical and thermal properties of magnetically aligned single wall carbon nanotube films. *Applied Physics Letters* 2000;**77**(5):666–8.
9. Thess A, Lee R, Nikolaev P, Dai H, Petit P, Robert J, et al. Crystalline ropes of metallic carbon nanotubes. *Science* 1996;**273**:483–7.
10. Barrera EV, Shofner ML, Corral EL. Applications: carbon nanotube composites. In: Meyyappan M, editor. *Carbon nanotubes in science and application*. New York: CRC Press; 2004.
11. Charlier J-C. Defects on carbon nanotubes. *Accounts of Chemical Research* 2002;**35**(12):1063–9.
12. Kataura H, Kumazawa Y, Maniwa Y, Ohtsuka Y, Sen R, Suzuki S, et al. Diameter control of single-walled carbon nanotubes. *Carbon* 2000;**38**(11–12):1691–7.
13. Meyyappan M. *Carbon nanotubes: science and application*. New York: CRC Press; 2005. pp. 289.
14. Corral EL, Cesarano J, Shyam A, Lara-Curzio E, Bell N, Stuecker J, et al. Engineered nanostructures for multifuntional single-walled carbon nanotube reinforced silicon nitride nanocomposites. *Journal of the American Ceramic Society* 2008;**91**(10):3129–37.

15. Yowell LL. *Thermal management in ceramics: synthesis and characterization of zirconia–carbon nanotube composite*. Houston: Department of Mechanical Engineering and Materials Science, Rice University; 2001. pp. 1–161.
16. Tatami J, Katashima T, Komeya K, Meguro T, Wakihara T. Electrically conductive Cnt-dispersed silicon nitride ceramics. *Journal of the American Ceramic Society* 2005;**88**(10):2889–93.
17. Poyato R, Vasiliev AL, Padture NP, Tanaka H, Nishimura T. Aqueous colloidal processing of single-wall carbon nanotubes and their composites with ceramics. *Nanotechnology* 2006;**17**:1770–7.
18. Sun J, Gao L, Wei Li. Colloidal processing of carbon nanotube/alumina composites. *Chemistry of Materials* 2002;**14**:5169–72.
19. Zhang S, Fahrenholtz W, Hilmas G. Pressureless sintering of carbon nanotube-Al_2O_3 composites. *Journal of the European* 2010;**30**:1373–80.
20. Israelachvili JN. *Intermolecular and surface forces*. London: Academic; 1992.
21. Zhan G-D, Kuntz JD, Wang H, Wang C-M, Mukherjee AK. Anisotropic thermal properties of single-wall-carbon-nanotube-reinforced nanoceramics. *Philosophical Magazine Letters* 2004;**84**(7):419–23.
22. Zhan G-D, Kuntz JD, Wan J, Mukherjee AK. Single-wall carbon nanotubes as attractive toughening agents in alumina based nanocomposites. *Nature Materials* 2003;**2**:38–42.
23. Zhan G-D, Kuntz JD, Garay JE, Mukherjee AK. Electrical properties of nanoceramics reinforced with ropes of single-walled carbon nanotubes. *Applied Physics Letters* 2003;**83**(6):1228–30.
24. Du H, Li Y, Zhou F, Su D, Hou F. One-step fabrication of ceramic and carbon nanotube (Cnt) composites by in situ growth of Cnts. *Journal of the American Ceramic Society* 2010;**9999**(9999).
25. Balani K, Zhang T, Karakoti A, Li W, Seal S, Agarwal A. In situ carbon nanotube reinforcements in a plasma-sprayed aluminum oxide nanocomposite coating. *Acta Materialia* 2008;**56**:571–9.
26. Balani K, Bakshi S, Chen Y, Laha T, Agarwal A. Role of powder treatment and carbon nanotube dispersion in the fracture toughening of plasma sprayed aluminum oxide-carbon nanotube composite. *Journal of Nanoscience and Nanotechnology* 2007;**7**:1–10.
27. Inam F, Yan H, Reece MJ, Peijs T. Dimethylformamide: an effective dispersant for making ceramic-carbon nanotube composites. *Nanotechnology* 2008;**19**:1–5.
28. Bakshi S, Balani K, Agarwal A. Thermal conductivity of plasma-sprayed aluminum oxide—multiwalled carbon nanotube composites. *Journal of the American Ceramic Society* 2008;**91**(3):942–7.
29. Sivakumar R, Guo S, Nishimura T, Kagawa Y. Thermal conductivity in multi-wall carbon nanotube/silica-based nanocomposites. *Scripta Materialia* 2007;**56**:265–8.
30. Balazsi C, Shen Z, Konya Z, Kasztovszky Z, Weber F, Vertesy Z, et al. Processing of carbon nanotube reinforced silicon nitride composites by spark plasma sintering. *Composites Science and Technology* 2005;**65**:727–33.
31. Belmonte M, González-Julián J, Miranzo P, Osendi MI. Spark plasma sintering: a powerful tool to develop new silicon nitride-based materials. *Journal of the European Ceramic Society* 2010;**30**(14):2937–46.
32. Belmonte M, Gonzalez-Julian J, Miranzo P, Osendi MI. Continuous in situ functionally graded silicon nitride materials. *Acta Materialia* 2009;**57**:2607–12.
33. Gazzara CP, Messier DR. Determination of phase content of Si_3N_4 by X-ray diffraction analysis. *American Ceramic Society Bulletin* 1977;**56**(9):777–80.
34. Rao AM, Richter E, Bandow S, Chase B, Eklund PC, Williams KW, et al. Diameter-selective raman scattering from vibrational modes in carbon nanotubes. *Science* 1998;**275**:187–91.
35. Dresselhaus MS, Dresselhaus G, Jorio A, Filho Souza AG, Pimenta MA, Saito R. Single nanotube Raman spectroscopy. *Accounts of Chemical Research* 2002;**35**(12):1070–8.
36. Ydaska M, Kataura H, Ichihashi T, Qin L-C, Kar S, Ijima S. Diameter enlargement of Hipco single-wall carbon nanotubes by heat treatment. *Nano Letters* 2001;**9**:487–9.
37. Hummel RE. *Electronic properties of materials*. New York: Springer-Verlag; 2000.
38. Zhan G-D, Kuntz JD, Wang H, Min Wang C, Mukherjee AK. Anisotropic thermal properties of single-wall-carbon-nanotube reinforced nanoceramics. *Philosophical Magazine Letters* 2004;**84**(7):419–23.
39. Torquato S, Rintoul MD. Effect of the interface on the properties of composite media. *Physics Review Letters* 1995;**75**(22):4067–70.
40. Issi JP. *Graphite and precursors*. New York: Gordon and Breech; 2001.
41. Koszor O, Lindemann A, Davin F, Balazsi C. Observation of thermophysical and tribological properties of CNT reinforced Si3N4. *Key Engineering Materials* 2009;**409**:354–7.